Anal. Chem. **2005,** *77,* 6528−6534

Determination of Ribonuclease H Surface Enzyme Kinetics by Surface Plasmon Resonance Imaging and Surface Plasmon Fluorescence Spectroscopy

Shiping Fang, Hye Jin Lee, Alastair W. Wark, Hyun Min Kim, and Robert M. Corn*

Department of Chemistry, University of California—Irvine, Irvine, California 92697

The kinetics of the ribonuclease H (RNase H) surface hydrolysis of RNA−DNA heteroduplexes formed on DNA microarrays was studied using a combination of real-time surface plasmon resonance imaging (SPRI) and surface plasmon fluorescence spectroscopy (SPFS). Time-dependent SPRI and SPFS data at various enzyme concentrations were quantitatively analyzed using a simple model that couples diffusion, enzyme adsorption, and surface enzyme kinetics. This model is characterized by a set of three rate constants, enzyme adsorption (k_a), enzyme desorption (k_d), enzyme catalysis (k_{cat}), and one dimensionless diffusion parameter (β). Values of $k_a = 3.15\ (\pm 0.20) \times 10^6\ M^{-1}\cdot s^{-1}$, $k_d = 0.10\ (\pm 0.05)\ s^{-1}$, and $k_{cat} = 0.95\ (\pm 0.10)\ s^{-1}$ were determined from fitting all of the SPRI and SPFS data sets. One of the most interesting kinetic parameters is the surface RNase H hydrolysis reaction rate constant (k_{cat}), which was found to be ~10 times slower than that observed in solution, but ~100 times faster than that recently observed for the exonuclease III surface hydrolysis of double-stranded DNA microarrays ($k_{cat} = 0.009\ s^{-1}$). Moreover, the surface coverage of the intermediate enzyme−substrate complex (ES) was found to be extremely small during the course of the reaction because k_{cat} is much larger than the product of k_a and the bulk enzyme concentration.

The incorporation of surface enzyme reactions into novel parallel biosensing methodologies that use biopolymer microarrays is an extremely effective method for increasing the sensitivity and specificity of these multielement surface bioaffinity measurements. The enzymatic processing of DNA, peptide, and protein microarrays is an attractive surface bioengineering tool for a number of reasons: surface enzyme reactions are highly specific and result in selective surface site modifications, work under biocompatible conditions with high efficiency, and can often be controlled with specific chemical cofactors. Examples of surface enzyme reactions currently implemented with multielement surface biosensors include single-nucleotide polymorphism detection with ligation and polymerase extension reactions[1] and the ultrasensitive detection of DNA with the ribonuclease H (RNase H) hydrolysis of RNA microarrays for enzymatically amplified surface plasmon resonance imaging (SPRI).[2,3] The characterization of the surface enzyme reactions that form the core of a particular biosensing process is of tantamount importance for optimization of the array biosensor since an enzyme reaction can be orders of magnitude slower on a surface as compared to solution due to a variety of transport and energetic factors.

So how does one completely characterize a surface enzyme reaction? Ideally, one should identify all of the surface species, reactants, intermediates, and products, and measure their surface coverages as a function of time. From this set of time-dependent surface coverage data, a model that describes the surface enzymatic process can then be constructed. SPRI is very good at measuring the adsorption and desorption of biomolecules onto surfaces[4−10] and can be used to provide some of this time-dependent surface coverage data.[11,12] However, since all surface species contribute to the SPRI signal, it is not possible to obtain a complete and independent set of kinetic surface coverage curves for each species; typically some assumptions must be made. A better methodology would be to label some of the surface species and use additional spectroscopic measurements to independently determine the various surface coverages. Surface plasmon fluorescence spectroscopy (SPFS) is a very sensitive fluorescence detection method that can detect fluorescently labeled molecules on gold thin films. Knoll et al. have used SPFS to detect a variety of surface biochemical interactions.[13−17] Using this technique with SPRI should allow us to obtain a more complete set of time-

* To whom correspondence should be addressed. E-mail: rcorn@uci.edu.

(1) Giusto, D. D.; King, G. C. *Nucleic Acids Res.* **2003**, *31*, e7.
(2) Goodrich, T. T.; Lee, H. J.; Corn, R. M. *J. Am. Chem. Soc.* **2004**, *126*, 4086−4087.
(3) Goodrich, T. T.; Lee, H. J.; Corn, R. M. *Anal. Chem.* **2004**, *76*, 6173−6178.
(4) Guedon, P.; Livache, T.; Martin, F.; Lesbre, F.; Roget, A.; Bidan, G.; Levy, Y. *Anal. Chem.* **2000**, *72*, 6003−6009.
(5) Wegner, G. J.; Lee, H. J.; Corn, R. M. *Anal. Chem.* **2002**, *74*, 5161−5168.
(6) Wegner, G. J.; Lee, H. J.; Marriott, G.; Corn, R. M. *Anal. Chem.* **2003**, *75*, 4740−4746.
(7) Smith, E. A.; Thomas, W. D.; Kiessling, L. L.; Corn, M. R. *J. Am. Chem. Soc.* **2003**, *125*, 6140−6148.
(8) Shumaker-Parry, J. S.; Campbell, C. T. *Anal. Chem.* **2004**, *76*, 907−917.
(9) Kanda, V.; Kariuki, J. K.; Harrison, D. J.; McDermott, M. T. *Anal. Chem.* **2004**, *76*, 7257−7262.
(10) Okumura, A.; Sato, Y.; Kyo, M.; Kawaguchi, H. *Anal. Biochem.* **2005**, *339*, 328−337.
(11) Wegner, G. J.; Wark, A. W.; Lee, H. J.; Codner, E.; Saeki, T.; Fang, S.; Corn, R. M. *Anal. Chem.* **2004**, *76*, 5677−5684.
(12) Lee, H. J.; Wark, A. W.; Goodrich, T. T.; Fang, S.; Corn, R. M. *Langmuir* **2005**, *21*, 4050−4057.
(13) Yu, F.; Persson, B.; Lofas, S.; Knoll, W. *J. Am. Chem. Soc.* **2004**, *126*, 8902−8903.
(14) Yu, F.; Yao, D.; Knoll, W. *Anal. Chem.* **2003**, *75*, 2610−2617.

10.1021/ac051283m CCC: $30.25
Published on Web 09/10/2005

dependent surface coverage measurements. Other researchers have realized the potential of this combination; for example, Robertson et al. have employed the combination of SPR and SPFS to characterize the reaction of protease on a monolayer of BSA.[18] In this paper, we will use the combination of SPRI and SPFS to measure time-dependent surface coverages in order to characterize the enzymatic hydrolysis of RNA in RNA−DNA heteroduplexes formed on a DNA microarray. It is this hydrolysis reaction that serves as the basis for the detection of DNA with enzymatically amplified SPRI measurements.[2,3]

Once the time-dependent surface coverage data have been obtained, one needs to choose a model to analyze the data. In a recent paper, we developed a simple model coupling diffusion, adsorption, desorption, and enzyme reaction kinetics that is a combination of Langmuir and Michaelis−Menten concepts.[12] We will use the same model here, where both the SPRI and SPFS time-dependent surface coverage data can be completely described by a set of three rate constants, k_a, k_d, and k_{cat}, and a mass transport coefficient k_m as shown in Figure 1.

THEORETICAL CONSIDERATIONS

A model that includes diffusion, adsorption, desorption, and the surface enzymatic reaction will be used to analyze the time-dependent SPRI and SPFS measurements of the surface hydrolysis of RNA−DNA heteroduplexes by RNase H. The overall reaction rate is controlled by the three processes shown in Figure 1: (i) mass transport of the enzyme (E) to the surface, (ii) the kinetics of adsorption and desorption of the enzyme onto a heteroduplex substrate (S) to form the surface enzyme−substrate complex (ES), and (iii) the surface hydrolysis of ES to form the surface ssDNA product S*. This reaction scheme can be written as eqs 1−3:

$$E_{(x=\infty)} \xrightarrow{k_m} E_{(x=0)} \tag{1}$$

$$S + E_{(x=0)} \underset{k_d}{\overset{k_a}{\rightleftharpoons}} ES \tag{2}$$

$$ES \xrightarrow{k_{cat}} S^* + E_{(x=0)} \tag{3}$$

where $E_{(x=\infty)}$ and $E_{(x=0)}$ are the bulk and surface enzyme species, respectively, k_m is the steady-state mass transport coefficient, S is the RNA−DNA surface-bound substrate (the RNA−DNA heteroduplex), ES is the surface enzyme−substrate complex (the RNase H−heteroduplex complex), k_a and k_d are the Langmuir adsorption and desorption rate constants, S* is the surface product (ssDNA), and k_{cat} is the surface reaction rate for the enzyme complex. The ratio k_a/k_d is the Langmuir adsorption coefficient K_{Ads}. The steady-state mass transport coefficient k_m can also be written as D/δ, where D is the diffusion coefficient for the enzyme and δ is the steady-state diffusion layer thickness.[19]

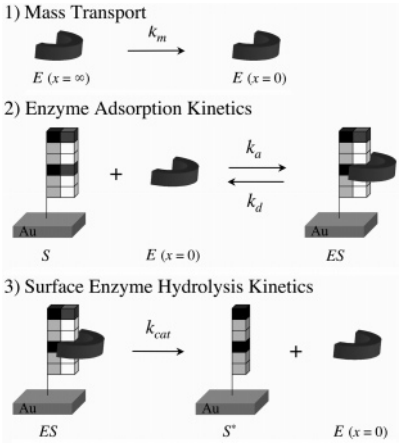

Figure 1. Reaction scheme showing the surface enzymatic processing of a biopolymer microarray including mass transport, enzyme adsorption onto a surface-bound substrate, and followed by a surface enzyme hydrolysis reaction.

This simplified scheme assumes that (i) we have created a stable RNA−DNA heteroduplex on the surface, (ii) there are only simple, noninteracting 1:1 substrate−enzyme surface complexes, and (iii) there is no adsorption of the enzyme E onto inactive surface areas. It is important to note that this reaction scheme is NOT the enzyme reaction mechanism typically used in the enzymatic detection of surface species in ELISA assays[20] or other related amplification schemes[21] because (i) the substrate and product are attached to the surface, (ii) the enzyme is only present as the surface complex ES, and (iii) the surface enzyme reaction releases the enzyme back into solution.

In a recent paper, we have derived the general differential kinetic equations that describe this surface enzyme reaction scheme.[12] If the surface coverages for the three surface species S, ES, and S* are denoted as Γ_S, Γ_{ES}, and Γ_{S^*}, respectively, and the total number of surface sites is Γ_{tot}, then the surface kinetics equations can be expressed in terms of the relative surface coverages $\theta_x = \Gamma_x/\Gamma_{tot}$,where x = S, ES, or S*:

$$\theta_S + \theta_{ES} + \theta_{S^*} = 1 \tag{4}$$

$$\frac{d\theta_{ES}}{dt} = \frac{k_a[E]^b(1 - \theta_{ES} - \theta_{S^*}) - (k_d + k_{cat})\theta_{ES}}{1 + \beta(1 - \theta_{ES} - \theta_{S^*})} \tag{5}$$

$$\frac{d\theta_{S^*}}{dt} = k_{cat}\theta_{ES} \tag{6}$$

In eq 5, $[E]^b$ is the bulk enzyme concentration and β is a dimensionless parameter[19,22] defined by eq 7:

$$\beta = \frac{k_a\Gamma_{tot}}{k_m} = \frac{k_a\Gamma_{tot}\delta}{D} \tag{7}$$

These equations were derived by assuming Langmuir adsorption/

(15) Yao, D.; Yu, F.; Kim, J.; Scholz, J.; Nielsen, P. E.; Sinner, E.; Knoll, W. *Nucleic Acids Res.* **2004**, *32*, e177.
(16) Tawa, K.; Knoll, W. *Nucleic Acids Res.* **2004**, *32*, 2372−2377.
(17) Stengel, G.; Knoll, W. *Nucleic Acids Res.* **2005**, *33*, e69.
(18) Kim, J.-H.; Roy, S.; Kellis, J. T., Jr.; Poulose, A. J.; Gast, A. P.; Robertson, C. R. *Langmuir* **2002**, *18*, 6312−6318.
(19) Bourdillon, C.; Demaille, C.; Moiroux, J.; Saveant, J. *J. Am. Chem. Soc.* **1999**, *121*, 2401−2408.
(20) Crowther, J. R. *ELISA: Theory and Practice*, 1st ed.; Humana Press Inc.: Totowa, NJ, 1995.
(21) He, L.; Musick, M. D.; Nicewarner, S. R.; Salinas, F. G.; Benkovic, S. J.; Natan, M. J.; Keating, C. D. *J. Am. Chem. Soc.* **2000**, *122*, 9071−9077.
(22) Schuck, P.; Minton, A. P. *Anal. Biochem.* **1996**, *240*, 262−272.

desorption kinetics and planar, steady-state diffusion to the surface that creates a constant diffusion layer in the flow cell microchannel.[23]

As shown in our previous paper, the general solution to these equations can be obtained by simple Euler integration methods and the initial conditions $\theta_S = 1$ and $\theta_{ES} = \theta_{S^*} = 0$. We will use computer-generated solutions to eqs 5 and 6 to fit our SPRI and SPFS measurements to obtain the four constants k_a, k_d, k_{cat}, and β. If the surface reaction is very slow ($k_{cat} \ll k_a[E]^b$) and diffusion can be neglected ($\beta = 0$), then a steady-state approximation for the surface enzyme coverage ($d\theta_{ES}/dt = 0$) can be used and a surface equivalent of the Michaelis−Menten equations can be derived.[12] These equations differ from the usual Michaelis−Menten equations in that the bulk enzyme concentration $[E]^b$ (and not the surface substrate coverage θ_S) controls the reaction rate.[24] In general, however, the steady-state approximation is NOT valid and the Michaelis−Menten equations cannot be used. In this case, k_{cat} is significant, and the surface reaction is normally run to completion where θ_S and θ_{ES} go to zero and θ_{S^*} goes to 1. Although θ_{ES} does not reach a steady-state value, we found previously that in all cases the fractional surface coverage of ES on the unreacted surface sites does reach a steady-state value.[12] This fractional surface coverage is defined as λ_{ES} and is given by eq 8:

$$\lambda_{ES} = \frac{\theta_{ES}}{\theta_{ES} + \theta_S} = \frac{\theta_{ES}}{1 - \theta_{S^*}} \tag{8}$$

If the surface reaction rate is very slow, this surface coverage is the same as the equilibrium surface coverage as determined from $[E]^b$ and the Langmuir adsorption coefficient.[12] As k_{cat} becomes large, λ_{ES} goes to zero. Once we have determined values of k_a, k_d, and k_{cat} from our data, we can calculate the steady-state value of λ_{ES} for the RNase H surface enzyme reaction using the following equation:

$$\lambda_{ES} = -\frac{k_a[E]^b}{k_{cat}\lambda_{ES}} + \frac{(k_a[E]^b + k_d + k_{cat})}{k_{cat}} \tag{9}$$

Equation 9 is a quadratic equation for the steady-state value of λ_{ES} that was derived in our previous paper[12] for the case $\beta = 0$; it also holds for $\beta \neq 0$.

EXPERIMENTAL SECTION

Materials. 11-Mercaptoundecylamine (MUAM, Dojindo), sulfosuccinimidyl 4-(*N*-maleimidomethyl)cyclohexane-1-carboxylate (SSMCC, Pierce), 9-fluorenylmethoxycarbonyl-*N*-hydroxysuccinimide (Fmoc-NHS, Novabiochem), *N*-hydroxysuccinimidyl ester of methoxypoly(ethylene glycol) propionic acid MW 2000 (PEG-NHS, Nektar Therapeutics), and RNase H (Takara Bio) were all used as received. Sterilized Tris buffer (50 mM Tris-HCl, 10 mM $MgCl_2$, 100 mM KCl, 10 mM DTT, 0.5 mM spermidine, pH 7.85) was used for DNA−RNA hybridization and all RNase H experiments. All rinsing steps were performed with absolute ethanol and autoclaved Millipore deionized water.

DNA and RNA Oligonucleotides. All the 5′-thiol-modified DNA oligonucleotides were purchased from Integrated DNA Technologies (IDT) and were deprotected and purified using binary reversed-phase HPLC. The thiol-modified DNA oligonucleotides used in these experiments are as follows: D1 = 5′-S−$S(CH_2)_6(T)_{20}$ CAC TGA GTC AGA GTC T-3′ and D2 = 5′-S−$S(CH_2)_6$ $(T)_{20}$ GTG TTA GCC TCA AGT G-3′. The HPLC purified complementary DNA sequence of D2 (C2 = 5′-CAC TTG AGG CTA ACA C-3′) was also purchased from IDT. All RNA oligonucleotides (RNase-free HPLC purified) were commercially obtained from Dharmacon RNA Technologies. The RNA sequences are as follows: R1 = 5′-AGA CUC UGA CUC AGU G-3′ and AFR1 = 5′- Alexa Fluor 647- AGA CUC UGA CUC AGU G-3′, which are both complementary to D1. 5′-Thiol-modified RNA R3 = 5′-HS-$(CH_2)_6(U)_8$ GUC AUU GCG ACU AGU G-3′ and its complementary RNA C3 = 5′-CAC UAG UCG CAA UGA C-3′.

Fabrication of DNA-Modified Gold Chips for SPFS and DNA Microarrays for SPRI. For both experiments, thin gold films (45 nm) with an underlayer of chromium (1 nm) were first deposited onto SF-10 glass slides (18 × 18 mm, Schott Glass) using a Denton DV-502A evaporator. The gold slide was then reacted with an amine-terminated self-assembled monolayer of MUAM (1 mM in ethanol) for a minimum of 4 h. For the DNA-modified gold chip used in SPFS measurements, the entire MUAM surface was modified with a heterobifunctional cross-linker, SSMCC (1 mM in 100 mM TEA, pH 7.0), by covering the chip surface with 500 μL of solution. This creates a thiol-reactive, maleimide-terminated surface. Next, 3 μL of 1 mM thiol-modified DNA solution was placed onto the SSMCC surface and spread over the whole surface by laying a cover glass against the gold slide overnight. Chip-to-chip variation was ∼5% for SFPS measurements. For the creation of DNA and RNA microarrays used in the SPRI measurements, two different methods were employed: (i) a multistep fabrication process described previously[25] for creating square patterns of arrays and (ii) a microchannel fabrication for the creation of line arrays.[26] In the former, the MUAM surface was reacted with the hydrophobic protecting group Fmoc-NHS. UV photopatterning of the MUAM surface with a quartz mask containing 500-μm square features created bare gold spots within the hydrophobic Fmoc background. The gold spots were then modified with MUAM and subsequently reacted with SSMCC. Thiol-modified sequences of DNA were then manually spotted onto the SSMCC array elements using a pneumatic picopump. The Fmoc background was then removed with a mildly basic solution to regenerate the MUAM surface. This surface was reacted with PEG-NHS (1 mM in 100 mM TEA, pH 8.0) to create a background that is resistant to nonspecific adsorption of biomolecules. For the line arrays utilized in all kinetic measurements,[11] a poly(dimethylsiloxane) (PDMS) microchannel (300-μm width, 14.2-mm length, 35-μm depth) with a 700-μm spacing between channels was placed onto the MUAM-modified gold surface. A solution of SSMCC was introduced to each channel using a simple aspiration pumping system. Solutions of thiol-

(23) Christensen, L. L. H. *Anal. Biochem.* **1997**, *249*, 153−164.
(24) Copeland, R. A. In *Enzymes: A practical introduction to structure, mechanism and data analysis*, 2nd ed.; Wiley-VCH: New York, 2000; pp 109−145.
(25) Brockman, J. M.; Frutos, A. G.; Corn, R. M. *J. Am. Chem. Soc.* **1999**, *121*, 8044−8051.
(26) Lee, H. J.; Goodrich, T. T.; Corn, R. M. *Anal. Chem.* **2001**, *73*, 5525−5531.

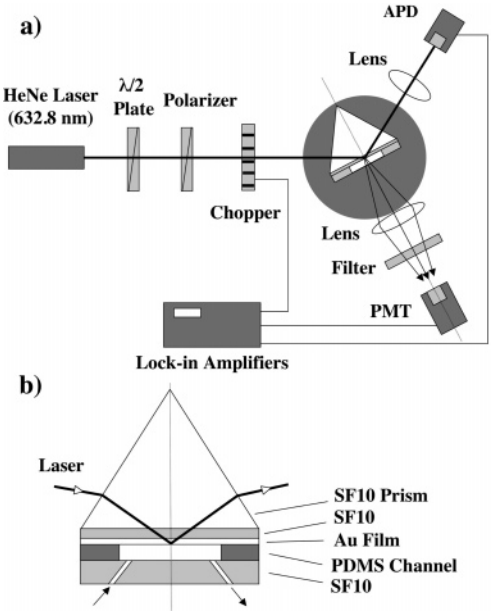

Figure 2. Schematic illustration of the SPR−SPFS experimental setup (a) and the prism/gold chip/flow cell assembly (b) used in SPFS measurements. A thin PDMS layer, fabricated by molding in an 800-μm-deep aluminum master, is sandwiched between the gold surface and a 1-mm-thick SF-10 transparent glass slide. The PDMS layer features a single 2-mm-wide microchannel, which runs diagonally across the chip surface. Entrance and exit holes were drilled through the backing SF-10 glass slide allowing the continuous delivery of buffer/sample through the channel using a syringe pump.

modified DNA probes (1 mM in 100 mM TEA, pH 7.0) were then introduced into each microchannel and left to react overnight. The PDMS microchannel was finally removed and the gold surface reacted with PEG-NHS.

SPFS Setup. A schematic showing the SPFS setup is depicted in Figure 2a. The output of a HeNe laser source (λ = 632.8 nm, 5 mW, Uniphase) is first collimated to achieve a beam diameter of 1.2 mm. The beam is then passed through a $\lambda/2$ wave plate and a polarizer to attenuate the laser power to ~2 μW where no photobleaching of the surface-bound dye was observed over the experimental time scale. Prior to incidence, the beam was modulated with a mechanical chopper at a frequency of 500 Hz. The reflected beam from the flow cell/gold chip/prism assembly was focused by a lens (f = 50 mm) onto an avalanche photodiode detector (C5460-01, Hamamatsu), which is connected to a lock-in amplifier (SR510, Standford Research Systems). The fluorescence emission from the labeled RNA hybridized onto the chip surface was collected from the back of the sample holder using a lens (Nikon, $f/\#$ = 1.2, f = 50 mm) and focused onto a photomultiplier tube (PMT, R928, Hamamatsu) via an interference filter (λ = 670 nm, $\Delta\lambda$ = 10 nm, 60% transmittance, Melles Griot). The signal output of the PMT was monitored with a second lock-in amplifier (EG&G 7220). The sample assembly was mounted on a rotation stage with all SPFS measurements performed at a fixed optimal angle, as defined in Figure 5. Data acquisition and control of the system was accomplished using custom programs written using Labview (National Instruments) software.

SPRI Measurements. An SPR imager (GWC Technologies) using near-infrared excitation from an incoherent white light source was used for all SPRI experiments. Briefly, a collimated p-polarized light is impinged onto a flow cell/gold chip/prism assembly at a fixed incident angle. The reflected light is directed through a band-pass filter (λ = 830 nm) and collected with a CCD camera. The data are collected using the software package V++ (Digital Optics). All kinetics experiments were obtained by collecting one data point for each region of interest approximately every 5 s that was the average of 30 camera frames. Kinetic data from multiple identical array elements were averaged to obtain the final SPRI response curves. All data processing and kinetic model fitting were performed using the software packages Microsoft Excel and Igor Pro. The details of the SPR imager and kinetic measurements can also be found elsewhere.[11]

Kinetic Flow Cell Design. For SPFS kinetic measurements, a thin PDMS layer, fabricated by molding in an 800-μm-deep aluminum master, is sandwiched between the gold surface and a 1-mm-thick SF-10 transparent glass slide (see Figure 2b). The PDMS layer features a single 2-mm-wide microchannel, which runs diagonally across the chip surface. Immediately prior to assembly, the PDMS layer was exposed to oxygen plasma for 10 s to improve the hydrophilicity of the inner channel walls and reduce nonspecific biomolecular adsorption. Entrance and exit holes were drilled through the backing SF-10 glass slide allowing the continuous delivery of buffer/sample through the channel using a syringe pump at a constant flow rate of 100 μL/min unless otherwise noted. The total flow cell volume was estimated to be ~34 μL. For SPRI kinetic measurements, a PDMS microfluidic system, described previously,[11] was used for the continuous delivery of small samples onto the array surface. Briefly, a serpentine PDMS microchannel (670-μm width, 9.5-cm total length, 200-μm depth, total volume ~10 μL) was pretreated with oxygen plasma and placed in direct contact with the gold surface. To reduce the fluctuations in SPR signal over time due to temperature and other environmental variations, a constant-temperature sample holder was used.[12] Solutions were delivered to the array surface using a syringe pump at a constant flow rate of 30 μL/min, and the temperature was controlled at 25 °C throughout the experiments.

RESULTS AND DISCUSSION

Using a combination of SPRI and SPFS measurements, we want to quantitatively measure the time dependence of the reaction of the enzyme RNase H with surface-bound RNA−DNA heteroduplexes. The process is depicted schematically in Figure 3. A 5′-thiol DNA oligonucleotide D1 (16 mer + 20 T spacer) was chemically attached to a maleimide-terminated alkanethiol monolayer on a gold surface as described previously.[25] Exposure of the surface to a 500 nM solution of a complementary RNA 16 mer (R1) led to the formation of RNA−DNA heteroduplexes on the surface. The surface was then exposed to a 30 units/mL (~8 nM) solution of RNase H for 5 min, which resulted in the removal of RNA from the surface.

SPRI Measurements. We have previously used SPRI of RNA microarrays to demonstrate the specificity of the RNase H surface hydrolysis reaction.[2,3] Also shown in Figure 3 is the SPR difference image of a three-component microarray (four replicate array elements for each component) before and after exposure to the RNase H solution. A significant loss in SPRI signal (−1.7% change in percent reflectivity, $\Delta\%R$) was observed due to the removal of R1 from the four D1 array elements. This $\Delta\%R$ loss was equal

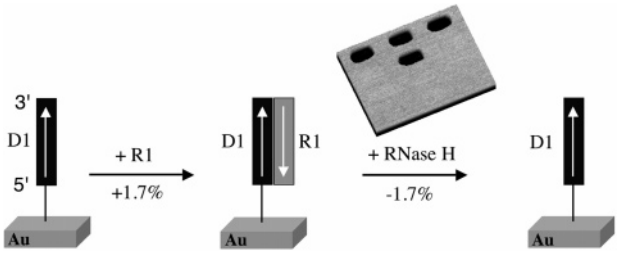

Figure 3. Schematic representation of RNase H hydrolysis of RNA from surface-bound RNA−DNA heteroduplexes. A 500 nM complementary RNA (R1) solution was exposed to a three-component DNA and RNA microarray. A reflectivity change of +1.7% was observed due to hybridization/adsorption of R1 to D1 array elements. Next, an 8 nM RNase H solution was introduced to the surface, which selectively hydrolyzes the complementary R1 sequence from R1−D1 heteroduplexes. The inset is the SPRI difference image obtained by subtracting images taken before and after the exposure of RNase H solution to the R1−D1 heteroduplexes and a reflectivity change of −1.7% was observed.

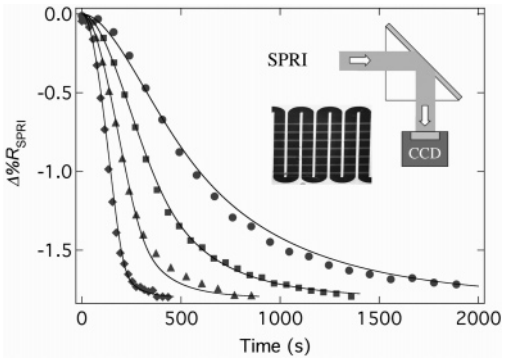

Figure 4. Time-dependent SPRI data obtained for the RNase H hydrolysis of surface RNA−DNA array elements at various concentrations of RNase H solutions (0.5 (●), 1.0 (■), 2.0 (▲), and 4.0 nM (◆)). All experimental curves were fitted using eqs 4−6 for all concentrations with the parameters $k_a = 3.4\ (\pm 0.2) \times 10^6\ M^{-1}\cdot s^{-1}$, $k_d = 0.10\ (\pm 0.05)\ s^{-1}$, $k_{cat} = 1.0\ (\pm 0.1)\ s^{-1}$, and $\beta = 180\ (\pm 20)$. The solid lines represent simulated kinetic curves. The inset shows a block diagram of the SPRI setup and an example of an SPRI raw image showing a serpentine PDMS channel placed perpendicular to DNA line arrays. This allows a uniform and continuous delivery of sample over each of the array elements.

and opposite to the +1.7% increase in $\Delta\%R$ observed upon hybridization of R1 to D1 (not shown), suggesting the complete removal of hybridized R1 from the surface. The other two components of the microarray in the SPR difference image contained double-stranded DNA (dsDNA, D2−C2) and dsRNA (R3−C3); neither of these duplexes was affected by RNase H, which reacts only with the heteroduplex. Also note that no adsorption of RNase H enzyme was observed on any of the array elements or background.

To quantitate the time dependence of the surface RNase H hydrolysis reaction, a series of real-time SPRI kinetic measurements were performed on a two-component DNA array in a microfluidic cell. Figure 4 shows the $\Delta\%R$ loss observed in the SPRI image at different enzyme concentrations ranging from 0.5 to 4 nM. A raw image of the microfluidic flow cell used in the measurements is shown in the inset of Figure 4; these real-time SPRI measurements have been described in detail previously.[3,11,12] The results in Figure 4 can be crudely quantitated by noting the time required to obtain half of the $\Delta\%R$ loss, defined as $T_{50\%}$, which ranged from 100 to 510 s (see Table 1).

Table 1. Summary of $T_{50\%}$ Values Obtained from SPRI and SPFS Kinetic Measurements at Different RNase H Concentrations[a]

concn of RNase H (nM)	$T_{50\%}$ (s) (SPRI)		$T_{50\%}$ (s) (SPFS)	
	exp	calc	exp	calc
0.5	510 (±5)	531 (±5)	910 (±20)	887 (±20)
1.0	314 (±15)	325 (±15)	591 (±15)	584 (±15)
2.0	200 (±5)	206 (±5)	405 (±10)	394 (±10)
4.0	130 (±5)	136 (±5)	286 (±7)	272 (±7)
8.0	95 (±3)	91 (±4)	195 (±5)	187 (±5)
16.0	58 (±2)	63 (±2)	133 (±3)	131 (±3)

[a] The experimental results are compared with those calculated using the k_a, k_d, k_{cat}, and β values detailed in Figures 4 and 6 for SPRI and SPFS, respectively.

The shape of the SPRI data in Figure 4 is qualitatively different from the real-time SPRI curves obtained in our previous studies of the surface hydrolysis of dsDNA by exonuclease III.[12] In those experiments, $\Delta\%R$ first rose positively before decaying to a steady-state negative value. This biphasic signal occurred because the SPRI data are the sum of all surface adsorption and desorption processes; in this case, both enzyme adsorption ($\theta_{ES}(t)$) and heteroduplex hydrolysis ($\theta_S(t)$). It is tempting to assume that because there is no increase in the $\Delta\%R$ curves in Figure 4, there is no significant surface coverage of enzyme ($\theta_{ES}(t) = 0$) during the RNase H hydrolysis reaction. However, it is possible that a small contribution from enzyme adsorption is present in Figure 4 that affects the $T_{50\%}$ times. To solve this ambiguity, we need to obtain an independent set of real-time SPFS data for the RNase H surface hydrolysis reaction.

SPFS Measurements. SPFS measurements were acquired using a special flow cell (34 μL total volume) designed to measure the SPFS and SPR responses simultaneously. For the SPFS measurements, a 5′-Alex fluor 647 RNA 16 mer (AFR1) was used to form the R1−D1 heteroduplex. The SPFS signal is therefore a direct measure of $\theta_S(t)$, and any loss in the SPFS signal during hydrolysis is due to the removal of fluorescently labeled target RNA from the surface. Prior to obtaining real-time kinetic data, both the SPFS and SPR signals were characterized as a function of incident laser angle as shown in Figure 5. Four-phase Fresnel calculations were used to fit both the SPR and SPFS data curves (http://corninfo.ps.uci.edu/calculations.html). As previously reported by Knoll,[27−29] the SPFS signal is largest near (but not precisely at) the SPR angle. All SPFS experiments were carried out at the SPFS angle (indicated by a dashed line in Figure 5) to achieve the maximum sensitivity of SPFS response. The SPR angle changed upon RNA hydrolysis by less than 0.1°,[30] so that there was no observable effect on the SPFS signal.

A series of real-time SPFS measurements for the RNase H hydrolysis reaction were performed at various concentrations

(27) Liebermann, T.; Knoll, W. *Colloids Surf. A* **2000**, *171*, 115−130.
(28) Liebermann, T.; Knoll, W.; Sluka, P.; Herrmann, R. *Colloids Surf. A* **2000**, *169*, 337−350.
(29) Neumann, T.; Johansson, M.; Kambhampati, D.; Knoll, W. *Adv. Funct. Mater.* **2002**, *12*, 575−586.
(30) Jordan, C. E.; Frutos, A. G.; Thiel, A. J.; Corn, R. M. *Anal. Chem.* **1997**, *69*, 4939−4947.

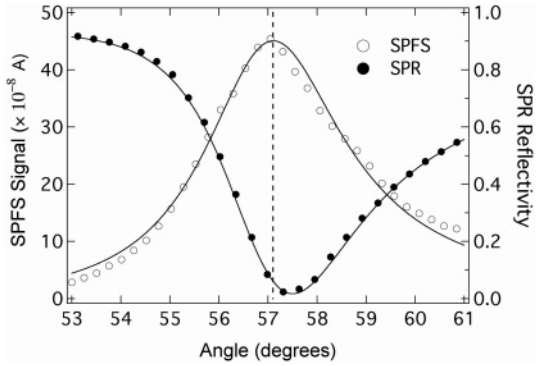

Figure 5. SPFS and SPR signals as a function of incident laser angle obtained for hybridization/adsorption of 500 nM fluorescently labeled RNA (AFR1) to surface-immobilized DNA (D1) probes. The SPR (●) and SPFS (○) curves were fitted using four-phase Fresnel calculations. The solid lines represent the fit. The dashed line corresponds to the angle position where the maximum fluorescence signal was achieved.

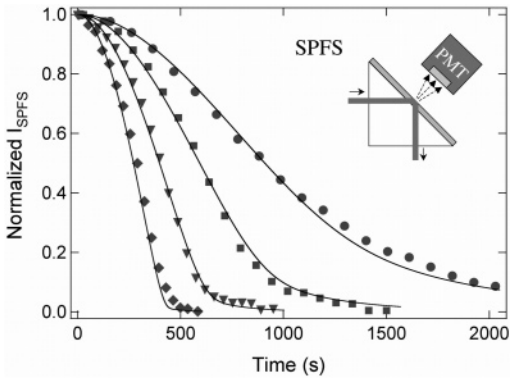

Figure 6. Time-dependent SPFS curves obtained for the surface RNase H hydrolysis of fluorescent RNA−DNA heteroduplexes at various concentrations of RNase H (0.5 (●), 1.0 (■), 2.0 (▼), and 4.0 nM (◆)). The solid lines represent the simulated kinetic curves fitted using eqs 4−6 with the parameters $k_a = 2.9\ (\pm 0.2) \times 10^6\ M^{-1}\cdot s^{-1}$, $k_d = 0.10\ (\pm 0.05)\ s^{-1}$, $k_{cat} = 0.9\ (\pm 0.1)\ s^{-1}$, and $\beta = 650\ (\pm 40)$. All the SPFS signals were normalized between zero and one with one corresponding to a full monolayer of AFR1−D1 heteroduplexes.

ranging from 0.5 to 4 nM and is shown in Figure 6. All the SPFS signals were normalized between zero and one with one corresponding to a full monolayer of AFR1−D1 heteroduplexes. An almost complete loss of fluorescence from the surface was observed upon completion of the hydrolysis reaction, implying that all of the RNA on the surface was accessible to the enzyme. The $T_{50\%}$ values for the SPFS data are listed in Table 1 and were slightly longer than those observed in the SPRI measurements (ranging from 300 to 900 s).

Kinetic Analysis. Since the SPFS signal is directly proportional to $\theta_S(t)$, we can use computer integration methods with eqs 4−6 to determine a best set of four constants (the three rate constants, k_a, k_d, and k_{cat}, and the diffusion parameter, β) that yields the best fit to the four SPFS curves obtained at different enzyme concentrations. The values for the four parameters are listed in Table 2, and the solid lines in Figure 6 are the fit to the data. Table 1 also summarizes $T_{50\%}$ values calculated using the same three rate constants. These values were in good agreement with the experimental values over the entire enzyme concentration range. The confidence intervals for k_{cat} and k_a are ∼10%, but the

Table 2. Values of the Three Rate Constants (k_a, k_d, k_{cat}) and the Diffusion Parameter (β) Determined from Fitting All the SPRI and SPFS Data Sets Using Eqs 4−6[a]

	k_a ($M^{-1}\cdot s^{-1}$)	k_d (s^{-1})	k_{cat} (s^{-1})	β
SPRI	3.40 (±0.20) × 10^6	0.10 (±0.05)	1.00 (±0.10)	180 (±20)
SPFS	2.90 (±0.20) × 10^6	0.10 (±0.05)	0.90 (±0.10)	650 (±40)
Avg.	3.15 (±0.20) × 10^6	0.10 (±0.05)	0.95 (±0.10)	n/a

[a] The data sets are shown in Figures 4 and 6.

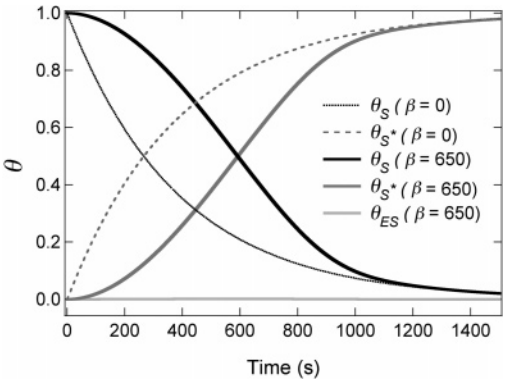

Figure 7. Kinetic simulation of the surface RNase H reactions defined in eqs 4−6. All simulation curves were obtained using 1 nM RNase H solution with the same rate constant values of k_a, k_d, and k_{cat} in Figure 6 for both $\beta = 0$ and $\beta = 650$.

uncertainty for k_d is higher (∼50%) because the surface coverage data are not as sensitive to this parameter. Using these constants, a complete set of time-dependent curves for $\theta_S(t)$, $\theta_{ES}(t)$, and $\theta_{S^*}(t)$ can be constructed and is shown in Figure 7.

A first key point in this kinetic analysis is that the SPFS data could not be fit without a nonzero β. This means that diffusional transport plays a role in the time dependence of the surface reaction. For comparison, the calculated curves for $\theta_S(t)$ and $\theta_{S^*}(t)$ when $\beta = 0$ are also shown in Figure 7. It is evident that the overall shape of $\theta_S(t)$ ($\beta = 0$) does not agree with any of the SPFS data. The value of β determined from the global fitting was 650 for a flow rate of 100 μL/min. The parameter β should vary with flow rate (proportional to $f^{-1/3}$);[23,31] β values of 1400 and 290 were obtained for flow rates of 10 and 1000 μL/min respectively, as predicted from theory. If we estimate the diffusion coefficient[31] for RNase H at $5 \times 10^{-6}\ cm^2\cdot s^{-1}$, from eq 7 and a β of 650, we can estimate a steady-state diffusion layer thickness of 100 μm for the 800-μm-deep flow cell at the flow rate of 100 μL/min.

A second key point in the kinetic analysis is that θ_{ES} is very small ($\sim 10^{-3}$). This means that the SPRI data are also directly proportional to $\theta_S(t)$ and can be fit in the same manner as the SPFS data. The values of the four fitting constants for the SPRI data are listed in Table 2; the kinetic rate constants are almost identical to those obtained from the SPFS data, indicating that the fluorescence labeling of RNA does not significantly affect k_{cat}. The only parameter that is significantly different is β, which is equal to 180. Since the SPRI measurements use a cell and flow

(31) Karlsson, R.; Roos, H.; Fagerstam, L.; Persson, B. *Methods: Companion Methods Enzymol.* **1994**, *6*, 99−110.

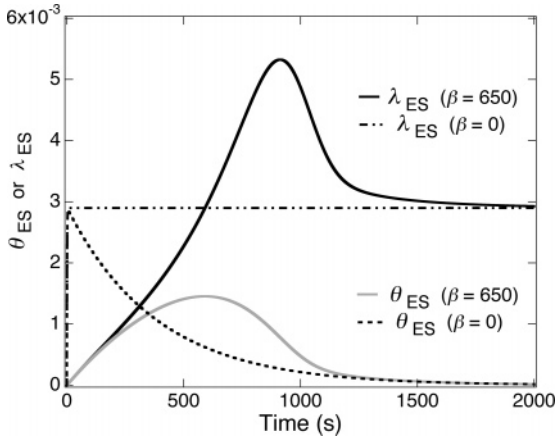

Figure 8. Theoretical analysis showing the time-dependent variations in the surface complex coverage (θ_{ES}) and the fraction of ES surface coverage on the unreacted surface sites (λ_{ES}). These were obtained using the same values of k_a, k_d, and k_{cat} reported in Figure 6 for both $\beta = 0$ and $\beta = 650$.

rate different from the SPFS measurement, a different β is expected.[31] From eq 7, a steady-state diffusion layer thickness of 28 μm for the 200-μm-deep SPRI flow cell is estimated.

Although $\theta_{ES}(t)$ is very small, the enzyme complex surface coverage is not equal to zero ($\theta_{ES} \neq 0$) and it changes during the course of the reaction ($d\theta_{ES}/dt \neq 0$). Figure 8 plots the enzyme complex surface coverage $\theta_{ES}(t)$ and the fractional enzyme surface coverage on unreacted sites $\lambda_{ES}(t)$ as predicted from our model for the case of 1 nM RNase H. As shown in our previous paper,[12] $\theta_{ES}(t)$ rises and then falls to zero through the course of the reaction, whereas $\lambda_{ES}(t)$ reaches a steady-state value that can be calculated from k_a, k_d, k_{cat} and $[E]^b$ to be 2.9×10^{-3}. Also shown in Figure 8 are $\theta_{ES}(t)$ and $\lambda_{ES}(t)$ for the case of $\beta = 0$. It is clear from this figure that the steady-state value for λ_{ES} does not depend on β, and agrees with the value of 2.9×10^{-3} calculated from eq 9.

A final point of the kinetic analysis is that the RNase H surface reaction is fast. The observed k_{cat} value of 0.95 s^{-1} is substantially larger than k_{cat} for the surface hydrolysis of dsDNA with Exo III (10^{-2} s^{-1}). Moreover, since $k_{cat} \gg k_a[E]^b$, it is easy to understand why θ_{ES} is very small: once adsorbed, the enzyme reacts very quickly and is released from the surface. Note that the condition $k_{cat} \gg k_a[E]^b$ is the complete opposite of the condition normally required for surface Michaelis–Menten kinetics ($k_{cat} \ll k_a[E]^b$), so those approximations cannot be used.[12] Last, although k_{cat} is large, it is still ~10 times slower than that observed in solution.[32,33] This suggests that k_{cat} may be improved by adding longer spacers to the surface-bound DNA to improve enzyme access to the substrate.

CONCLUSIONS

In this paper, we have shown that the combination of real-time SPRI and SPFS measurements can be used to obtain the time-dependent surface coverage data required in the analysis of the RNase H–heteroduplex surface hydrolysis reaction on DNA microarrays. These data were incorporated into a simple model of coupled biomolecular adsorption and surface enzyme kinetics characterized by three rate constants, k_a, k_d, and k_{cat}, and a diffusion parameter, β. All of the SPRI and SPFS data could be successfully fit with one set of surface rate constants. The value for the surface hydrolysis reaction rate constant (k_{cat}) of 0.95 s^{-1} is ~10 times smaller than that observed in solution. However, it is ~100 times faster than the exonuclease III–dsDNA surface hydrolysis rate observed previously.[12] Throughout the course of the RNase H surface reaction, the surface enzyme–substrate complex coverage (θ_{ES}) remains very small due to this rate constant ($k_{cat} \gg k_a[E]^b$). Surface enzyme kinetics serves as the foundation of many enzyme-related surface biotechnologies, and the work presented here shows unequivocally the utility of the combination of SPRI and SPFS in the analysis of these surface biosensing systems. We will examine the kinetics of other surface enzyme reactions used in biosensing methodologies in future papers.

ACKNOWLEDGMENT

This research is funded by the National Institute of Health (2RO1 GM059622-04) and the National Science Foundation (CHE-0133151). The authors thank Dr. Terry T. Goodrich for obtaining the SPR difference image shown in Figure 3.

Received for review July 20, 2005. Accepted August 22, 2005.

AC051283M

(32) Hogrefe, H. H.; Hogrefe, R. I.; Walder, R. Y.; Walder, J. A. *J. Biol. Chem.* **1990**, *265*, 5561–5566.
(33) Keck, J. L.; Goedken, E. R.; Marqusee, S. *J. Biol. Chem.* **1998**, *273*, 34128–34133.